



Published in final edited form as:

Stem Cells. 2012 October ; 30(10): 2100–2113. doi:10.1002/stem.1193.

ALDH1A Isozymes Are Markers of Human Melanoma Stem Cells and Potential Therapeutic Targets

Yuchun Luo^a, Katuscia Dallaglio^{a,b}, Ying Chen^c, William A Robinson^d, Steven E Robinson^d, Martin D McCarter^e, Jianbin Wang^f, Rene Gonzalez^d, David C Thompson^g, David A Norris^{a,h}, Dennis R Roop^{a,b}, Vasilis Vasilidou^c, and Mayumi Fujita^{a,b,h}

^aDepartment of Dermatology, University of Colorado Denver, Aurora, CO 80045, USA

^bCharles C Gates Center for Regenerative Medicine and Stem Cell Biology, University of Colorado Denver, Aurora, CO 80045, USA

^cDepartment of Pharmaceutical Sciences, University of Colorado Denver, Aurora, CO 80045, USA

^dDivision of Medical Oncology, Department of Medicine, University of Colorado Denver, Aurora, CO 80045, USA

^eDepartment of Surgery, University of Colorado Denver, Aurora, CO 80045, USA

^fDepartment of Biochemistry and Molecular Genetics, University of Colorado Denver, Aurora, CO 80045, USA

^gClinical Pharmacy, University of Colorado Denver, Aurora, CO 80045, USA

^hDenver Veterans Affairs Medical Center, Denver, CO 80220

Abstract

Although the concept of cancer stem cells (CSCs) is well accepted for many tumors, the existence of such cells in human melanoma has been the subject of debate. In the present study, we demonstrate the existence of human melanoma cells that fulfill the criteria for CSCs (self-renewal and differentiation) by serially xenotransplanting cells into NOD/SCID mice. These cells possess high aldehyde dehydrogenase (ALDH) activity with ALDH1A1 and ALDH1A3 being the predominant ALDH isozymes. ALDH-positive melanoma cells are more tumorigenic than ALDH-negative cells in both NOD/SCID mice and NSG mice. Biological analyses of the ALDH-positive melanoma cells reveal the ALDH isozymes to be key molecules regulating the function of these cells. Silencing ALDH1A by siRNA or shRNA leads to cell cycle arrest, apoptosis and decreased cell viability *in vitro* and reduced tumorigenesis *in vivo*. ALDH-positive melanoma cells are more resistant to chemotherapeutic agents and silencing ALDH1A by siRNA sensitizes melanoma cells to drug-induced cell death. Furthermore, we, for the first time, examined the molecular signatures of ALDH-positive CSCs from patient-derived tumor specimens. The signatures of melanoma

Correspondence: Mayumi Fujita, MD, PhD, Department of Dermatology, University of Colorado Denver, Mail Stop 8127, 12801 E. 17th Ave., Rm 4124, Aurora, CO 80045, USA. Phone 303-724-4045. Fax 303-724-4048. mayumi.fujita@ucdenver.edu.

DISCLOSURE OF POTENTIAL CONFLICTS OF INTEREST

The authors disclosed no potential conflicts of interest.

Author Contributions:

Y.L.: conception and design, collection and assembly of data, data analysis and interpretation, manuscript writing, and final approval of manuscript; K.D., Y.C., J.W.: collection and assembly of data, data analysis and interpretation, and final approval of manuscript; W.A.R., S.E.R., M.D.M., R.G.: provision of study material or patients, and final approval of manuscript; D.C.T., D.A.N., D.R.R., V.V.: data analysis and interpretation, and final approval of manuscript; M.F.: conception and design, financial support, collection and assembly of data, data analysis and interpretation, manuscript writing, and final approval of manuscript.

CSCs include retinoic acid (RA)-driven target genes with RA response elements and genes associated with stem cell function. These findings implicate that ALDH isozymes are not only biomarkers of CSCs but also attractive therapeutic targets for human melanoma. Further investigation of these isozymes and genes will enhance our understanding of the molecular mechanisms governing CSCs and reveal new molecular targets for therapeutic intervention of cancer.

Keywords

melanoma; cancer stem cells; tumor initiating cells; aldehyde dehydrogenase; microarray analysis; molecular targeted therapy

INTRODUCTION

Increasing evidence indicates that cancer cells with stem cell-like properties have a potential for self-renewal and differentiation, thereby driving tumorigenesis [1]. Although this cancer stem cell (CSC) hypothesis has been supported by numerous studies in solid tumors over the past decade, the existence of CSCs in human melanoma has been the subject of considerable debate. Initially, stem cell-like subpopulations of human melanoma cells were reported to be enriched in CD20⁺ cells [2] and CD133⁺ cells [3]. Subsequent studies identified CSCs from human melanoma using ABCB5, a member of the ATP-binding cassette (ABC) transporter family [4], and CD271 [5]. These cells fulfill the criteria for CSCs, namely “self-renewal (or serially transplantable)” and “differentiation (i.e., generating heterogeneous lineages recapitulating an original tumor)” [6]. However, the existence of CSCs in human melanoma has been questioned because it was reported that as many as 1 in 4 human melanoma cells were tumorigenic and that none of the 22 heterogeneously expressed cell surface markers (including ABCB5 and CD271) correlated with tumorigenic capacity in highly permissive xenotransplantation condition using nonobese diabetic/severe combined immunodeficiency (NOD/SCID) interleukin-2 receptor γ -chain-null (NSG) mice [7, 8].

Recognizing the limitations associated with relying on stem cell surface markers that may be vulnerable to CSC isolation procedures, we sought to use intracellular markers of stem cells in human melanoma. Aldehyde dehydrogenases (ALDHs) are a superfamily of detoxifying enzymes. ALDH isozymes metabolize a wide variety of intracellular aldehydes and can thus provide resistance to alkylating chemicals such as cyclophosphamide [9, 10]. High ALDH activities have been reported in hematopoietic, neural and prostate stem cells [11–16] as well as CSCs from many cancers including those found in breast, lung, liver, colon, pancreatic, ovarian, head and neck and prostate [17–30]. In human melanoma, however, the role of ALDH in tumorigenesis has been controversial; while one report could not find an association between ALDH activity and enhanced tumor initiation in melanoma [31], another study reported selection of tumorigenic melanoma cells using ALDH [32]. Neither study analyzed the self-renewal capacity of ALDH-positive (ALDH⁺) cells by serially transplanting these cells into mice, an important criterion for CSCs. More importantly, although ALDH has been implicated as a marker of CSCs, it is not yet known how ALDH contributes to the phenotypes and functions of CSCs or whether ALDH can be used for CSC-directed therapy.

In the present study, we investigated tumor-initiating capacity and CSC properties of human melanoma tumors. We demonstrate that high ALDH activity identifies CSCs in human melanoma. We provide evidence that ALDH isozymes are not only markers of CSCs but they also regulate the biological behaviors of CSCs. Accordingly, ALDH isozymes may serve as potential therapeutic targets.

MATERIALS AND METHODS

Patient Melanoma Specimens

Human melanoma tumors were provided by the University of Colorado Hospital from surgical specimens with written informed consent by patients under Institutional Review Board-approved protocols, adhering to Health Insurance Portability and Accountability Act Regulations. Tumors were processed for histological and biological analyses (see below). Parts of the fresh melanoma tissues were implanted into subcutaneous pockets made by a small incision on the flank of 5- to 6-week-old female athymic (*nu/nu*) mice (NCI) for establishing direct *in vivo* xenograft model [33, 34]. Patient tumors and xenografted tumors in the first or second generation were used in this study (Supplemental Table 1). Animal experiments were performed under the institutional guidelines for the use of laboratory animals.

Tumor Cell Isolation

Patient tumors and xenografted tumors were minced with a surgical blade and single cell suspensions were generated by enzymatic digestion with 1 mg/ml (235 U/ml) collagenase I (Sigma-Aldrich) and 1 mg/ml (850 U/ml) hyaluronidase (Sigma-Aldrich) for 2 hours at 37°C with intermittent vortexing, followed by sequentially passage through 70- and 40- μ m filters (Fisher Scientific). Red blood cells were lysed using 1 \times Red Blood Cell Lysis Buffer (eBioscience). Cells were washed twice and subjected to FACS.

Aldefluor[®] Assay and Fluorescence-activated Cell Sorting (FACS)

The Aldefluor[®] kit (Stem Cell Technologies) was used to isolate cells with high ALDH activity. Briefly, cells were suspended in Aldefluor[®] assay buffer containing BODIPY-aminoacetaldehyde and incubated at 37°C for 30 minutes. Control samples were incubated with the buffer containing 50 mM diethylaminobenzaldehyde (DEAB), an ALDH inhibitor. To eliminate human stromal cells from tumors obtained from patients, we used phycoerythrin-cy7-labeled anti-human CD45 (eBioscience) and anti-human CD31 (eBioscience) antibodies. To eliminate mouse cells from xenografted tumors, we used allophycocyanin-labeled anti-mouse MHC class I (H-2K^d, eBioscience), phycoerythrin-cy7-labeled anti-mouse CD45 (eBioscience) and anti-mouse CD31 (eBioscience) antibodies. DAPI (Sigma-Aldrich) was used to eliminate dead cells. Cell sorting was conducted using a MoFlo machine (DakoCytomation) and the results were analyzed using Summit software (DakoCytomation). The Aldefluor[®] staining was detected using the FITC channel. To prevent cross-contamination between ALDH⁺ and ALDH⁻ cells, sorting gates of these 2 populations were set up at least one log apart. The purity of sorted populations was re-analyzed using ALDH⁺ and ALDH⁻ cells and was shown to be greater than 95%.

Tumorigenicity in Immunodeficient Mice

Sorted cells were suspended in 100 μ l of the culture medium containing 50% standard matrigel (product 354234; BD Biosciences). Intradermal injection of cells was performed on the flanks of 6–8 week old NOD/SCID mice (NCI) or NSG mice (Jackson Laboratories). Tumor size was measured once a week by caliper. Tumor volume was calculated by the formula: tumor volume = (longest diameter) \times (shortest diameter)²/2. Frequency of tumor-initiating cells (TICs) was calculated using L-Calc Software (Stem Cell Technologies) and significance was determined by chi-square analysis.

Microarray Analysis

Total RNA (5 ng) was amplified using NuGEN WT-Ovation[™] Pico system (NuGEN Technologies) according to the manufacturers' instructions. cRNA was hybridized using

standard Illumina protocols to Human HT-12 v3 Expression Beadchips (Illumina) containing more than 25,000 genes with 48,804 entities/probes. Signal intensity values were generated by Illumina Beadstudio version 2 software. The median average intensity for all samples was normalized and rescaled by the BeadStudio software with recommended parameters. GeneSpringGX Version 10.0 (Agilent Technologies) was used for normalization of one-color array data with default threshold to remove transcripts with low or negative expression values (i.e., value < 1) from the data. Raw data were filtered on expression with setting of upper (100) and lower (20.0) percentile cut-offs, and filtered on flags present or marginal, retaining 42,786 entities. Statistical analysis was performed by ANOVA using Illumina microarray system. A sample tree was generated from the clustering of values with Euclidean distance analyzed by GeneSpringGX 10.0.

ALDH mRNA Copy Number Analysis

RNA was reverse transcribed using random primers and MMLV reverse transcriptase (Promega). Real-time quantitative reverse transcription-PCR (qRT-PCR) of ALDH genes was performed in an ABI-PRISM 7000 Sequence Detection System (Applied Biosystems) using the Power SYBR Green PCR Master Mix (Applied Biosystems). Ten ng of RNA was used in each qRT-PCR reaction and duplicates were run for each sample. Individual ALDH mRNA abundance was quantified by fitting qRT-PCR data to a standard curve generated from a cDNA construct of the gene. Briefly, a previously generated construct containing the cDNA sequence of individual ALDH gene was used as the cDNA templates (3, 30, 300, 3,000, 30,000, 300,000 copies/reaction) by serial dilution in the qRT-PCR reaction to develop a standard curve. The mass of one plasmid molecule was calculated as mass (g/copy) = plasmid size (bp) \times 1.096×10^{-21} (g/bp) (www.appliedbiosystems.com). The data were reported as copy numbers (or copies) of mRNA molecule per ng RNA for individual ALDH genes. The primers used in this assay are summarized in Supplemental Table 2.

Retinoic Acid Response Elements (RAREs) Analysis

The -10 kb to +1 kb sequences of the transcription start site of the genes were obtained from the PromoSer (<http://biowulf.bu.edu/zlab/PromoSer/>). The RARE motifs [(A/G)G(G/T)TCA(n) (A/G)G(G/T)TCA, n = 1, 2 or 5] were searched from both forward and reverse strand of these sequences using an in-house Perl script, which is available on request.

Other Methods

Further information about the materials and methods used in this work are provided in the Supplementary Materials and Methods online section.

RESULTS

Human Melanoma Tumors Contain Cells with High ALDH Activity

We obtained 12 tumors from melanoma patients. We analyzed ALDH activity by Aldefluor[®] assay using 9 patient tumors (3 primary and 6 metastatic) and 10 xenografted tumors from a direct *in vivo* xenograft model (4 primary and 6 metastatic) (Supplemental Table 1). Eight of 9 patient tumors and 8 of 10 xenografted tumors harbored small and discrete ALDH⁺ subpopulations, ranging from 0.08% to 1.15% of all live melanoma cells (discrete pattern) (Supplemental Table 1 and Fig. 1A, *upper and middle panels*). One of 9 patient tumors (MB952) and 2 of 10 xenografted tumors (MB952 and MB1009) contained > 10% of ALDH⁺ cells, which were not distinct from the main cell population and merged with other cells in the sample without clear segregation (shift pattern) (Fig. 1A, *lower panel*). Whereas biological differences between two patterns are unknown, a discrete pattern was observed in both primary and metastatic melanomas and a shift pattern was observed

only in metastatic melanoma. These data confirm the presence of ALDH⁺ cells in human melanoma.

ALDH⁺ Melanoma Cells Display CSC Properties *in vivo*

We investigated the tumor initiating capability of ALDH⁺, ALDH-negative (ALDH⁻) and the corresponding parental cells *in vivo*. Because of limited quantities of fresh tumor tissues, we used tumors from a direct *in vivo* xenograft model [33, 34]. Cells were isolated by FACS from 6 xenografted melanomas (MF347, MB929, MB947p, MB947m, MB952 and MB1009) (Table 1A). ALDH⁺, ALDH⁻ and parental cells showed no statistical differences in cell viability *in vitro* (Fig. 1B); however, ALDH⁺ cells formed tumors much faster than ALDH⁻ and parental tumors after intradermal injection in NOD/SCID mice (Fig. 1C). To avoid underestimating TIC frequency by a short observation time, all mice were monitored for up to 24 weeks. Whereas 100 ALDH⁺ cells formed tumors at 18 out of 21 sites (85.7%), 100 ALDH⁻ cells and parental cells formed tumors at 2 out of 21 sites (9.5%) and 7 out of 21 sites (33.3%), respectively (Table 1A). When 10 cells were injected, only ALDH⁺ cells formed tumors (3/12 or 25%). The frequency of TICs was considerably higher in ALDH⁺ cells (1 in 150) than ALDH⁻ cells (1 in 2,910, $P < 1e^{-12}$ compared to ALDH⁺ cells) or parental cells (1 in 520, $P = 0.0004$ compared to ALDH⁺ cells), indicating that ALDH⁺ melanoma cells were enriched with TICs (Table 1A). A comparison of primary and metastatic melanoma cells from the same patient revealed that TIC frequency was increased 10-fold in the metastatic melanoma (1 in 1,650 in MB947p parental cells versus 1 in 165 in MB947m parental cells, $P < 0.05$).

Next, we investigated whether ALDH⁺ cells and/or ALDH⁻ cells possess the CSC properties of self-renewal and differentiation. Tumors from ALDH⁺ and ALDH⁻ cells were serially transplanted into NOD/SCID mice (Table 1B). Whereas secondary and tertiary tumors were observed from 1,000 ALDH⁺ cells from ALDH⁺ tumors (MF347, MB947p and MB1009), 1,000 ALDH⁻ cells from ALDH⁻ tumors (MB947p and MB1009) failed to form palpable tumors during the 24 weeks of observation time, confirming a self-renewal capacity of ALDH⁺ cells. No statistical differences were observed for TIC frequency in ALDH⁺ cells from the primary, secondary and tertiary tumors (1 in 150, <155, and <663, respectively). We then analyzed the ability of ALDH⁺ cells and ALDH⁻ cells to differentiate under *in vitro* and *in vivo* conditions. Whereas ALDH⁺ cells showed a tendency to differentiate to ALDH⁻ cells, ALDH⁻ cells retained the ALDH⁻ phenotype *in vitro* (Fig. 1D). Similar results were obtained *in vivo* such that tumors generated from ALDH⁺ cells re-established tumor heterogeneity by producing both ALDH⁺ and ALDH⁻ cells whereas tumors generated from ALDH⁻ cells comprised of only ALDH⁻ cells (Fig. 1E). Furthermore, tumors generated from ALDH⁺ cells maintained proportions of ALDH⁺ and ALDH⁻ cells comparable to those found in their original tumors (Fig. 1E, 1F). All together, these findings demonstrate that ALDH⁺ human melanoma cells fulfill the criteria for CSCs, *viz* self-renewal and differentiation.

Recent studies have reported a high frequency of TICs in human melanoma when tumor cells were xenotransplanted in NSG mice [7, 8]. These studies did not identify a marker that could distinguish tumorigenic and nontumorigenic melanoma cells in this highly permissive xenotransplantation condition. However, ALDH isozymes were not investigated in the studies. Therefore, limiting dilutions (1000, 100 and 10 cells) of ALDH⁺ and ALDH⁻ cells from 2 xenografted melanomas (MF347 and MB952) were injected intradermally into NOD/SCID mice and NSG mice (Table 1C). Consistent with previous reports showing higher tumorigenicity in NSG mice, TIC frequency of ALDH⁻ cells was approximately 10-fold high in NSG mice (1 in 8,370 in NOD/SCID mice versus 1 in 830 in NSG mice, $P = 0.136$). However, ALDH⁺ cells were equally tumorigenic in NOD/SCID and NSG mice (TIC frequency was 1 in 100 in both mice, $P = 1$). When tumorigenicity was compared in NSG

mice, ALDH⁺ cells exhibited a statistically higher TIC frequency than ALDH⁻ cells (1 in 100 versus 1 in 830, $P=0.016$), supporting our conclusion that ALDH activity can distinguish tumorigenic and nontumorigenic melanoma cells in both NOD/SCID mice and NSG mice.

ALDH1A1 and ALDH1A3 Are the Predominant ALDH Isozymes Expressed in ALDH⁺ Subpopulation of Human Melanoma Tumors

Because ALDH⁺ human melanoma cells were enriched with CSCs, we speculated that these cells may have unique molecular signatures, thereby conferring enhanced and sustained tumorigenic properties. We first examined which ALDH isozymes are responsible for the strong Aldefluor[®] staining in ALDH⁺ melanoma cells. The human ALDH superfamily includes 19 family members [9, 35], with individual ALDH member displays unique tissue distribution, subcellular localization and substrate specificity [36]. Microarray analysis of ALDH⁺ and ALDH⁻ cells from xenografted tumors (MF347, MB929 and MB947m) revealed that seventeen ALDH genes were upregulated and 2 genes were downregulated in ALDH⁺ cells (Fig. 2A), verifying the accuracy of an Aldefluor[®] isolation methodology. Of those upregulated isozymes, ALDH⁺ cells expressed over 15-fold more ALDH1A1 and ALDH1A3 than ALDH⁻ cells. To further investigate the absolute abundance of the different ALDH isozymes, we examined the mRNA copy number for 7 representative ALDH family members using 5 xenografted tumors (MF347, MB929, MB947p, MB947m and MB952) (Fig. 2B). We observed great individual variations in expression among these tumors. In general, ALDH1A1 was the most abundant ALDH isozyme in ALDH⁺ cells from xenografted melanomas with an average mRNA copy number of 337 per ng RNA. ALDH1A3 was ranked second with an average mRNA copy number of 29 per ng RNA. ALDH⁺ cells from MF347 and MB952 expressed both ALDH1A1 (45 and 61 copies per ng RNA in MF347 and MB952, respectively) and ALDH1A3 (107 and 32 copies per ng RNA in MF347 and MB952, respectively). ALDH⁺ cells from other 3 tumors (MB929, MB947p and MB947m) expressed ALDH1A1 predominantly and very little ALDH1A3 (< 3 copies per ng RNA). The average copy numbers of the other 5 ALDH isozymes (ALDH1A2, 1B1, 3A1, 3B1 and 4A1) were below 5 per ng RNA. Immunohistochemical stainings of ALDH1A1 and ALDH1A3 were consistent with the mRNA findings (Fig. 2C).

Silencing the ALDH1A Genes Leads to Cell Cycle Arrest, Apoptosis and Decreased Viability of ALDH⁺ Human Melanoma Cells

Considering the enhanced and sustained tumorigenic property of ALDH⁺ melanoma cells, we investigated whether downregulating ALDH activity could alter the biological behavior of ALDH⁺ human melanoma cells. Although the most appropriate source of cells to address this question would be fresh patient tumor cells or cells from xenografted melanomas, the limited quantity of these cells makes biological experiments challenging. Therefore, we performed experiments using human melanoma cell lines first, and then verified pertinent findings using xenografted patient tumors.

Analysis of mRNA copy number in human melanoma cell lines revealed that ALDH1A3 was much more abundant (over 200-fold) than ALDH1A1 in ALDH⁺ cells (Supplemental Fig. 1). Transfection of ALDH⁺1205Lu cells and ALDH⁺A375 cells with either ALDH1A3-#1 or ALDH1A3-#2 siRNAs led to a reduction of ALDH1A3 mRNA expression (87% or 88% reduction in ALDH⁺1205Lu cells, and 86% or 89% reduction in ALDH⁺A375 cells, respectively), along with a concordant reduction in ALDH1A3 protein expression (Fig. 3A). Because ALDH1A3-#1 and ALDH1A3-#2 siRNAs produced an equivalent level of repression of mRNA expression, we used only ALDH1A3-#1 siRNA in subsequent experiments. Repressing ALDH1A3 resulted in a reduction of ALDH enzymatic activity in ALDH⁺1205Lu and ALDH⁺A375 cells (Fig. 3B). Cell cycle analysis revealed an

accumulation of cells in G1 phase (21.4% increase in ALDH⁺1205Lu cells and 14.1% increase in ALDH⁺A375 cells) and a reduction of cells in S phase (50.6% decrease in ALDH⁺1205Lu cells and 14.3% decrease in ALDH⁺A375 cells) (Fig. 3C). Furthermore, ALDH1A3 knockdown induced apoptosis (4.0-fold increase in ALDH⁺1205Lu cells and 2.8-fold increase in ALDH⁺A375 cells 72 hours after transfection compared with control siRNA transfection) (Fig. 3D). We then investigated the effect of ALDH1A3 knockdown on cell viability. Compared with control siRNA, transfection with ALDH1A3 siRNA led to 54% and 55% decreases in cell viability in ALDH⁺1205Lu cells and ALDH⁺A375 cells, respectively (Fig. 3E).

Next, we analyzed patient tumor cells to verify these results. We used MB952 tumor because this tumor contained >10% ALDH⁺ cells and expressed both ALDH1A1 and ALDH1A3. Transfection of ALDH1A1-#1 and ALDH1A3-#1 siRNAs into ALDH⁺ cells from MB952 cells led to reductions of ALDH1A1 and ALDH1A3 mRNA expression by 71% and 90%, respectively (Fig. 3F), along with reductions in cell viability by 65% and 68%, respectively (Fig. 3G). These results confirm the findings from the cell lines.

Targeting ALDH1A Isozymes by shRNAs Inhibits Tumor Growth *in vivo*

To test whether ALDH1A family isozymes were responsible for tumor growth *in vivo*, we silenced ALDH1A in ALDH⁺1205Lu cells, and subsequently implanted the transfected cells intradermally into NOD/SCID mice. Because ALDH1A3 is much more abundant than ALDH1A1 in ALDH⁺1205Lu cells, only ALDH1A3 was knocked down. GFP-shRNAs were used for sustainable effects and selection of successful transfectants by sorting (Supplemental Fig. 2). As shown in Fig. 3H, a significant reduction in tumor growth was observed in ALDH⁺1205Lu cells transfected with ALDH1A3 shRNA compared with their corresponding shRNA control group. Histological analysis revealed that tumors from ALDH1A3 knockdown cells contained many apoptotic cells, fewer mitotic cells and reduced ALDH1A3 expression than control tumors. These results support the notion that ALDH activity is critical for cell survival and tumor growth.

ALDH⁺ Melanoma Cells Are Resistant to Chemotherapy and Silencing the ALDH1A Genes Sensitizes Melanoma Cells to Drug- Induced Cell Death

CSCs have been shown to be resistant to various drugs [37]. To examine the drug resistance of human melanoma cells, we treated 1205Lu cells and A375 cells with various chemotherapeutics. Temozolomide is an alkylating agent used in the treatment of melanoma [38]. Paclitaxel has shown to have positive outcomes in phase II/III clinical trials of melanoma [39, 40]. Doxorubicin is a widely used chemotherapeutic agent but relatively ineffective against melanoma [41]. All three treatments resulted in an increase in ALDH1A3 expression (56.7%, 30.4% or 162% increase in 1205Lu cells and 112%, 343% or 662% increase in A375 cells after treatment with temozolomide, paclitaxel or doxorubicin, respectively) (Fig. 4A), suggesting an association between the ALDH level and drug-response/sensitivity. We then investigated the relative chemoresistance of ALDH⁺ cells and ALDH⁻ cells by treating them separately with temozolomide, paclitaxel or doxorubicin. As shown in Fig. 4B, ALDH⁺1205Lu cells and ALDH⁺A375 cells showed decreased sensitivity to these drugs than ALDH⁻1205Lu cells and ALDH⁻ A375 cells, respectively. To address if silencing ALDH1A expression alters chemoresistance in ALDH⁺ cells, we analyzed drug-induced cytotoxicity after knockdown of ALDH1A3 in ALDH⁺1205Lu cells and ALDH⁺A375 cells. Both apoptotic and necrotic cell deaths were measured. Transfection of ALDH1A3 siRNA led to increased cytotoxicity when cells were treated with temozolomide (2.6-fold and 1.5-fold in ALDH⁺1205Lu cells and ALDH⁺A375 cells, respectively), paclitaxel (1.6-fold and 2.5-fold in ALDH⁺1205Lu cells and ALDH⁺A375 cells, respectively) or doxorubicin (1.6-fold and 1.3-fold in ALDH⁺1205Lu cells and

ALDH⁺A375 cells, respectively) (Fig. 4C). These findings suggest that the expression of ALDH1A genes contributes to the chemoresistance in ALDH⁺ melanoma cells.

Profiling of ALDH⁺ and ALDH⁻ Subpopulations Identifies Retinoic Acid (RA)-Driven Target Genes with RA Response Elements and Genes Associated with Stem Cell Function

To understand the biology of ALDH⁺ human melanoma cells, we analyzed differentially expressed genes in ALDH⁺ cells using microarray data. Unsupervised hierarchical cluster analysis applied to the 6 samples (ALDH⁺ and ALDH⁻ cells from MF347, MB947m, MB929 tumors) and 42,786 filtered entities did not separate ALDH⁺ and ALDH⁻ samples. However, supervised hierarchical clustering of 1,196 entities differentially expressed between ALDH⁺ and ALDH⁻ samples ($P < 0.05$, fold change > 2.0 by asymptomatic two-way ANOVA) led to a clear separation of these 2 groups, suggesting that only a limited number of genes are differentially expressed between ALDH⁺ and ALDH⁻ samples (Supplemental Fig. 3). A more stringent selection criterion (fold change > 5.0 , $P < 0.05$) identified 285 entities including 147 annotated genes that were differentially expressed between ALDH⁺ and ALDH⁻ groups (Table 2, Fig. 5A). Among 99 upregulated genes in ALDH⁺ cells, 7 were known stem cell genes (*ADAR*, *ALDH1A3*, *CCNB3*, *CDC42*, *DACH1*, *FGF6* and *FOXP1*) and 13 genes were potentially associated with stem cell functions, such as cell cycle, mitosis, cell proliferation and anti-apoptosis (Table 2). The remainder of the upregulated genes were involved in a variety of biological processes, including transporters, protein binding, regulation of transcription, signal transduction, metabolic processes and cell adhesion. On the other hand, many downregulated genes in ALDH⁺ cells were potentially associated with lineage-specific development, differentiation, apoptosis and negative regulation of angiogenesis.

ALDH1A isozymes oxidize retinaldehyde to RA. RA regulates the expression of a variety of genes through nuclear receptors (RAR and RXR) which control the transcription of target genes by interacting with specific DNA sequences, RA response elements (RAREs) [42]. RAREs are located in the promoter region of target genes and consist of 2 core hexameric motifs, PuG(G/T)TCA, separated by 1, 2 or 5 spacer nucleotides [42, 43]. To identify RA-driven target genes, we searched RARE motifs in 147 genes (Table 2). Twenty-four genes were not analyzed because their sequences in the region -10 kb to $+1$ kb from transcription start were not determined by PromoSer. Among 123 genes analyzed, we identified 67 RAREs from 45 genes. Thirty-seven RAREs were from the coding strand and 30 RAREs were from the non-coding strand, and 89.5% of the RAREs had 2 spacer nucleotides (Supplemental Table 3). Whereas a third of genes in each functional category contained RAREs, only one gene (*CDC42*) out of 9 stem cell genes contained RAREs.

Gene expression of three upregulated genes in ALDH⁺ cells were validated by qRT-PCR: *CDC42*, a stem cell gene with RAREs, (3.1-fold in MF347 and 1.2-fold in MB929); *ADAR*, a stem cell gene without RAREs, (3.1-fold in MF347 and 2.9-fold in MB929); and *USH1C*, a potential stem cell gene without RAREs, (27.5-fold in MF347 and 3.0-fold in MB929) (Fig. 5B). These findings were further confirmed using 1205Lu cells (Supplemental Fig. 4A). To address whether silencing of ALDH1A alters levels of differentially expressed genes in ALDH⁺ cells, we analyzed the three upregulated genes after knockdown of ALDH1A1 and ALDH1A3 in ALDH⁺ cells from MB952 tumor. Transfection of ALDH1A1 siRNA failed to significantly affect expression of *ADAR*, *CDC42* or *USH1C*, although there was a trend to a reduction in *USH1C* (40% reduction). Transfection of ALDH1A3 siRNA had no effect on *ADAR* but it resulted in 72% and 75% suppression of *CDC42* and *USH1C* mRNAs, respectively (Fig. 5C). These findings were further confirmed using 1205Lu cells, which showed 83% and 98% reduction in *CDC42* and *USH1C* mRNA, respectively, but no significant alteration in *ADAR* after transfection with ALDH1A3 siRNA (Supplemental Fig. 4B). These results illustrate that some stem cell genes are controlled by the ALDH1A3

isozyme, and help unravel the crucial role of ALDH activity on proliferation and survival of human melanoma CSCs.

DISCUSSION

In the present study, we confirm the existence of cells that fulfill the criteria for CSCs in the patient-derived human melanoma cells. These cells possess high ALDH activity. We demonstrate that ALDH⁺ human melanoma cells are more tumorigenic than ALDH⁻ cells in both NOD/SCID mice and NSG mice. In contrast to ALDH⁻ melanoma cells that displayed increased tumorigenesis in NSG mice compared with NOD/SCID mice, ALDH⁺ cells were equally tumorigenic in NOD/SCID and NSG mice. The main difference between these mouse strains is the presence of NK cells in NOD/SCID mice, and these results indicate that NK cells suppress the tumor growth of ALDH⁻ cells in NOD/SCID mice while they have little impact on the tumorigenesis of ALDH⁺ cells. This may represent an immunoevasive phenotype of ALDH⁺ cells, a property that would contribute to the enhanced tumorigenic properties of ALDH⁺ cells beyond their intrinsic tumorigenic ability. Compared with ALDH⁻ cells, ALDH⁺ cells expressed lower levels of melanocyte differentiation antigens, MLANA (MART-1) and TYRP1 (TRP-1) (Fig. 5D), which would further contribute to an immunoevasive phenotype of ALDH⁺ cells. Whether ALDH⁺ melanoma CSCs and previously reported melanoma CSCs (ABC5⁺ [4] or CD271⁺ [5]) are distinct or overlapping populations warrants further investigation. Our preliminary studies suggest some overlap occurs among these populations (Fig. 5E).

It was reported that the frequency of melanoma TICs was dramatically increased in NSG mice as opposed to NOD/SCID mice [7, 8]. Whereas these studies showed that as many as 1 in 4 unselected human melanoma cells formed tumors, the TIC frequency of ALDH⁻ cells in our study was 1 in 830 in NSG mice. The more tumorigenic ALDH⁺ melanoma cells also failed to form tumors at such a high frequency in NSG mice. Four other groups have been unable to show a high frequency of tumorigenic cells from human melanoma tumors [5, 32, 46] or other cancers [47] in NSG mice. These discrepancies may be explained in part by variations in the methodologies used for dissociation and isolation of cancer cells, xenotransplantation experiments and source of tumor materials [48–50].

Considering the strong association between ALDH activity and CSCs, it is important to identify the ALDH isoforms responsible for high ALDH activity and characterize the molecular signatures expressed in ALDH⁺ cells. The human ALDH1A subfamily contains ALDH1A1, ALDH1A2 and ALDH1A3 enzymes [36, 51]. The ALDH1A1 has been considered to be the key isozyme for the positive Aldefluor[®] staining [16]. However, it is not unreasonable to speculate that the isozyme expressed in each cancer type could differ because the expression of ALDH isozymes is organ- and tissue-specific [36]. By combining microarray and qRT-PCR analysis, we have demonstrated that ALDH1A1 is the most abundant isoform in ALDH⁺ cells in human melanoma whereas ALDH1A3 is the most abundant isoform in ALDH⁺ cells from melanoma cell lines. We have also found that some patient tumors express both ALDH1A1 and ALDH1A3 in the ALDH⁺ subpopulation. Recent studies have revealed the association between Aldefluor[®] staining and expression of ALDH1A1 and ALDH1A3 in human breast CSCs [45, 52]. Together with the present results, these findings indicate that, in addition to ALDH1A1, ALDH1A3 may be a novel marker for certain types of CSCs. Furthermore, we provide evidence that ALDH1A isozymes in human melanomas are essential to the function of CSCs and may serve as therapeutic targets. By silencing ALDH1A1 and ALDH1A3, we demonstrated a significant decrease in cell viability and an increase in apoptosis in ALDH⁺ human melanoma cells *in vitro*. This was also confirmed by reduced tumorigenesis *in vivo* after knockdown of ALDH1A. Furthermore, ALDH⁺ human melanoma cells were resistant to chemotherapeutic

agents, and we showed that their resistance was attributed to the expression of ALDH1A genes. These findings strongly suggest that ALDH isozymes may not simply serve as CSC markers but they are the key molecules governing cell proliferation, survival and chemoresistance of CSCs.

Despite their important roles in CSCs, the molecular mechanisms of ALDH isozymes in CSCs have not been well understood. ALDH isozymes are involved in the synthesis of RA, betaine and carnitine, and through such mechanisms, may function as key enzymes in pathways associated with cell proliferation, differentiation and survival [36, 51, 53]. Indeed, we demonstrated that many genes identified from microarray analysis are RA-driven target genes with RAREs. We confirmed that the expression of *CDC42*, a gene with 3 RAREs, was regulated by the ALDH1A isozymes whereas that of *ADAR*, a gene without RAREs, was not. Interestingly, we also found that the expression of *USH1C*, a gene without RAREs, was regulated by the ALDH1A isozymes. These data suggest that ALDH1A isozymes contribute to the stemness of human melanoma CSCs through RA-dependent and -independent pathways. In addition to RA signaling, the capacity of ALDH to metabolize cytotoxic aldehydes (arising endogenously or as a result of chemotherapy, radiation or oxidative stress) would be a key determinant for the survival and drug resistance of cancer cells. Thus, further investigation of ALDH1A isozymes and genes differentially expressed in ALDH⁺ CSCs are clearly warranted. Eradicating stem-like cancer components must be an essential part of cancer treatment in addition to eliminating non-stem cancer cells [54], and suppression of these isozymes and genes by specific small molecules may be a promising modality for CSC-directed therapeutics in human melanoma.

CONCLUSION

In conclusion, the present study has demonstrated that cancer cells with CSC properties exist in ALDH⁺ human melanoma cells. We have identified ALDH isozymes and characterized the molecular signatures and biological properties associated with the ALDH isozymes. We provide evidence that ALDH1A isozymes are not only markers of CSCs but also important in cell survival, proliferation and chemoresistance of CSCs. These functions make the ALDH isozymes novel and attractive therapeutic targets for human melanoma. To the best of our knowledge, this is the first study to examine the molecular signatures of ALDH⁺ CSCs using patient-derived tumors. Further investigation of these isozymes and genes will enhance our understanding of the molecular mechanisms governing CSCs and reveal new molecular targets for designing anticancer drugs.

Supplementary Material

Refer to Web version on PubMed Central for supplementary material.

Acknowledgments

We thank the University of Colorado Denver (UCD) melanoma tissue bank for providing human melanoma samples, the University of Colorado Cancer Center (UCCC) flow core (Alistaire S. Acosta and Karen Helm) for helping with FACS sorting, the Mind Research Network from New Mexico (Marilee Morgan and Kent Hutchison) for helping with microarray analysis, and Garrick Talmage for assisting with experiments. We also thank Miki Tanioka, MD, PhD (Department of Dermatology, Kyoto University) and J Daniel Jensen, MD (Sacred Heart Medical Center from Spokane, WA) for critically reviewing the manuscript. This work was supported by an NIH grant CA125833 (to M.F.), Veterans Affairs Merit Review Award (to M.F.), a grant from the UCCC (to M.F.), Wendy Will Case Cancer Fund (to M.F.), Tadimitsu Cancer Research Fund (to M.F.) and NEI grants EY17963 & EY11490 (to V.V.).

References

1. Reya T, Morrison SJ, Clarke MF, et al. Stem cells, cancer, and cancer stem cells. *Nature*. 2001; 414:105–111. [PubMed: 11689955]
2. Fang D, Nguyen TK, Leishear K, et al. A tumorigenic subpopulation with stem cell properties in melanomas. *Cancer Res*. 2005; 65:9328–9337. [PubMed: 16230395]
3. Monzani E, Facchetti F, Galmozzi E, et al. Melanoma contains CD133 and ABCG2 positive cells with enhanced tumorigenic potential. *Eur J Cancer*. 2007; 43:935–946. [PubMed: 17320377]
4. Schatton T, Murphy GF, Frank NY, et al. Identification of cells initiating human melanomas. *Nature*. 2008; 451:345–349. [PubMed: 18202660]
5. Boiko AD, Razorenova OV, van de Rijn M, et al. Human melanoma-initiating cells express neural crest nerve growth factor receptor CD271. *Nature*. 2010; 466:133–137. [PubMed: 20596026]
6. Clarke MF, Dick JE, Dirks PB, et al. Cancer stem cells—perspectives on current status and future directions: AACR Workshop on cancer stem cells. *Cancer Res*. 2006; 66:9339–9344. [PubMed: 16990346]
7. Quintana E, Shackleton M, Sabel MS, et al. Efficient tumour formation by single human melanoma cells. *Nature*. 2008; 456:593–598. [PubMed: 19052619]
8. Quintana E, Shackleton M, Foster HR, et al. Phenotypic heterogeneity among tumorigenic melanoma cells from patients that is reversible and not hierarchically organized. *Cancer Cell*. 2010; 18:510–523. [PubMed: 21075313]
9. Sophos NA, Vasiliou V. Aldehyde dehydrogenase gene superfamily: the 2002 update. *Chem Biol Interact*. 2003; 143–144:5–22.
10. Magni M, Shammah S, Schiro R, et al. Induction of cyclophosphamide-resistance by aldehyde dehydrogenase gene transfer. *Blood*. 1996; 87:1097–1103. [PubMed: 8562935]
11. Armstrong L, Stojkovic M, Dimmick I, et al. Phenotypic characterization of murine primitive hematopoietic progenitor cells isolated on basis of aldehyde dehydrogenase activity. *Stem Cells*. 2004; 22:1142–1151. [PubMed: 15579635]
12. Hess DA, Meyerrose TE, Wirthlin L, et al. Functional characterization of highly purified human hematopoietic repopulating cells isolated according to aldehyde dehydrogenase activity. *Blood*. 2004; 104:1648–1655. [PubMed: 15178579]
13. Hess DA, Wirthlin L, Craft TP, et al. Selection based on CD133 and high aldehyde dehydrogenase activity isolates long-term reconstituting human hematopoietic stem cells. *Blood*. 2006; 107:2162–2169. [PubMed: 16269619]
14. Corti S, Locatelli F, Papadimitriou D, et al. Identification of a primitive brain-derived neural stem cell population based on aldehyde dehydrogenase activity. *Stem Cells*. 2006; 24:975–985. [PubMed: 16293577]
15. Levi BP, Yilmaz OH, Duester G, et al. Aldehyde dehydrogenase 1a1 is dispensable for stem cell function in the mouse hematopoietic and nervous systems. *Blood*. 2009; 113:1670–1680. [PubMed: 18971422]
16. Burger PE, Gupta R, Xiong X, et al. High aldehyde dehydrogenase activity: a novel functional marker of murine prostate stem/progenitor cells. *Stem Cells*. 2009; 27:2220–2228. [PubMed: 19544409]
17. Todaro M, Iovino F, Eterno V, et al. Tumorigenic and metastatic activity of human thyroid cancer stem cells. *Cancer Res*. 2010; 70:8874–8885. [PubMed: 20959469]
18. Ucar D, Cogle CR, Zucali JR, et al. Aldehyde dehydrogenase activity as a functional marker for lung cancer. *Chem Biol Interact*. 2009; 178:48–55. [PubMed: 18952074]
19. Jiang F, Qiu Q, Khanna A, et al. Aldehyde dehydrogenase 1 is a tumor stem cell-associated marker in lung cancer. *Mol Cancer Res*. 2009; 7:330–338. [PubMed: 19276181]
20. van den Hoogen C, van der Horst G, Cheung H, et al. High aldehyde dehydrogenase activity identifies tumor-initiating and metastasis-initiating cells in human prostate cancer. *Cancer Res*. 2010; 70:5163–5173. [PubMed: 20516116]
21. Rasheed ZA, Yang J, Wang Q, et al. Prognostic significance of tumorigenic cells with mesenchymal features in pancreatic adenocarcinoma. *J Natl Cancer Inst*. 2010; 102:340–351. [PubMed: 20164446]

22. Wang L, Park P, Zhang H, et al. Prospective identification of tumorigenic osteosarcoma cancer stem cells in OS99-1 cells based on high aldehyde dehydrogenase activity. *Int J Cancer*. 2010
23. Clay MR, Tabor M, Owen JH, et al. Single-marker identification of head and neck squamous cell carcinoma cancer stem cells with aldehyde dehydrogenase. *Head Neck*. 2010
24. Croker AK, Goodale D, Chu J, et al. High aldehyde dehydrogenase and expression of cancer stem cell markers selects for breast cancer cells with enhanced malignant and metastatic ability. *J Cell Mol Med*. 2009; 13:2236–2252. [PubMed: 18681906]
25. Ginestier C, Hur MH, Charafe-Jauffret E, et al. ALDH1 is a marker of normal and malignant human mammary stem cells and a predictor of poor clinical outcome. *Cell Stem Cell*. 2007; 1:555–567. [PubMed: 18371393]
26. Carpentino JE, Hynes MJ, Appelman HD, et al. Aldehyde dehydrogenase-expressing colon stem cells contribute to tumorigenesis in the transition from colitis to cancer. *Cancer Res*. 2009; 69:8208–8215. [PubMed: 19808966]
27. Chen YC, Chen YW, Hsu HS, et al. Aldehyde dehydrogenase 1 is a putative marker for cancer stem cells in head and neck squamous cancer. *Biochem Biophys Res Commun*. 2009; 385:307–313. [PubMed: 19450560]
28. Charafe-Jauffret E, Ginestier C, Iovino F, et al. Aldehyde dehydrogenase 1-positive cancer stem cells mediate metastasis and poor clinical outcome in inflammatory breast cancer. *Clin Cancer Res*. 2009; 16:45–55. [PubMed: 20028757]
29. Dylla SJ, Beviglia L, Park IK, et al. Colorectal cancer stem cells are enriched in xenogeneic tumors following chemotherapy. *PLoS One*. 2008; 3:e2428. [PubMed: 18560594]
30. Silva IA, Bai S, McLean K, et al. Aldehyde dehydrogenase in combination with CD133 defines angiogenic ovarian cancer stem cells that portend poor patient survival. *Cancer Res*. 2011; 71:3991–4001. [PubMed: 21498635]
31. Prasmickaite L, Engesaeter BO, Skrbo N, et al. Aldehyde dehydrogenase (ALDH) activity does not select for cells with enhanced aggressive properties in malignant melanoma. *PLoS One*. 2010; 5:e10731. [PubMed: 20505780]
32. Boonyaratanakornkit JB, Yue L, Strachan LR, et al. Selection of tumorigenic melanoma cells using ALDH. *J Invest Dermatol*. 2010; 130:2799–2808. [PubMed: 20739950]
33. Luo Y, Ellis LZ, Dallaglio K, et al. Side Population Cells from Human Melanoma Tumors Reveal Diverse Mechanisms for Chemoresistance. *J Invest Dermatol*. 2012
34. Rubio-Viqueira B, Jimeno A, Cusatis G, et al. An in vivo platform for translational drug development in pancreatic cancer. *Clin Cancer Res*. 2006; 12:4652–4661. [PubMed: 16899615]
35. Vasiliou V, Nebert DW. Analysis and update of the human aldehyde dehydrogenase (ALDH) gene family. *Hum Genomics*. 2005; 2:138–143. [PubMed: 16004729]
36. Marchitti SA, Brocker C, Stagos D, et al. Non-P450 aldehyde oxidizing enzymes: the aldehyde dehydrogenase superfamily. *Expert Opin Drug Metab Toxicol*. 2008; 4:697–720. [PubMed: 18611112]
37. Eyler CE, Rich JN. Survival of the fittest: cancer stem cells in therapeutic resistance and angiogenesis. *J Clin Oncol*. 2008; 26:2839–2845. [PubMed: 18539962]
38. Bleehen NM, Newlands ES, Lee SM, et al. Cancer Research Campaign phase II trial of temozolomide in metastatic melanoma. *J Clin Oncol*. 1995; 13:910–913. [PubMed: 7707118]
39. Bedikian AY, Plager C, Papadopoulos N, et al. Phase II evaluation of paclitaxel by short intravenous infusion in metastatic melanoma. *Melanoma Res*. 2004; 14:63–66. [PubMed: 15091196]
40. Hauschild A, Agarwala SS, Trefzer U, et al. Results of a phase III, randomized, placebo-controlled study of sorafenib in combination with carboplatin and paclitaxel as second-line treatment in patients with unresectable stage III or stage IV melanoma. *J Clin Oncol*. 2009; 27:2823–2830. [PubMed: 19349552]
41. Vorobiof DA, Rapoport BL, Mahomed R, et al. Phase II study of pegylated liposomal doxorubicin in patients with metastatic malignant melanoma failing standard chemotherapy treatment. *Melanoma Res*. 2003; 13:201–203. [PubMed: 12690306]
42. Leid M, Kastner P, Chambon P. Multiplicity generates diversity in the retinoic acid signalling pathways. *Trends Biochem Sci*. 1992; 17:427–433. [PubMed: 1333659]

43. Balmer JE, Blomhoff R. A robust characterization of retinoic acid response elements based on a comparison of sites in three species. *J Steroid Biochem Mol Biol.* 2005; 96:347–354. [PubMed: 16081280]
44. Huang EH, Hynes MJ, Zhang T, et al. Aldehyde dehydrogenase 1 is a marker for normal and malignant human colonic stem cells (SC) and tracks SC overpopulation during colon tumorigenesis. *Cancer Res.* 2009; 69:3382–3389. [PubMed: 19336570]
45. Charafe-Jauffret E, Ginestier C, Iovino F, et al. Breast cancer cell lines contain functional cancer stem cells with metastatic capacity and a distinct molecular signature. *Cancer Res.* 2009; 69:1302–1313. [PubMed: 19190339]
46. Frank NY, Schatton T, Kim S, et al. VEGFR-1 Expressed by Malignant Melanoma-Initiating Cells Is Required for Tumor Growth. *Cancer Res.* 2011; 71:1474–1485. [PubMed: 21212411]
47. Ishizawa K, Rasheed ZA, Karisch R, et al. Tumor-initiating cells are rare in many human tumors. *Cell Stem Cell.* 2010; 7:279–282. [PubMed: 20804964]
48. Girouard SD, Murphy GF. Melanoma stem cells: not rare, but well done. *Lab Invest.* 2011; 91:647–664. [PubMed: 21445060]
49. Civenni G, Walter A, Kobert N, et al. Human CD271-positive melanoma stem cells associated with metastasis establish tumor heterogeneity and long-term growth. *Cancer Res.* 2011; 71:3098–3109. [PubMed: 21393506]
50. Ghadially R. The role of stem and circulating cells in cancer metastasis. *J Surg Oncol.* 2011; 103:555–557. [PubMed: 21480249]
51. Chute JP, Muramoto GG, Whitesides J, et al. Inhibition of aldehyde dehydrogenase and retinoid signaling induces the expansion of human hematopoietic stem cells. *Proc Natl Acad Sci U S A.* 2006; 103:11707–11712. [PubMed: 16857736]
52. Marcatò P, Dean CA, Pan D, et al. Aldehyde dehydrogenase activity of breast cancer stem cells is primarily due to isoform ALDH1A3 and its expression is predictive of metastasis. *Stem Cells.* 2011; 29:32–45. [PubMed: 21280157]
53. Pares X, Farres J, Kedishvili N, et al. Medium- and short-chain dehydrogenase/reductase gene and protein families : Medium-chain and short-chain dehydrogenases/reductases in retinoid metabolism. *Cell Mol Life Sci.* 2008; 65:3936–3949. [PubMed: 19011747]
54. Jordan CT, Guzman ML, Noble M. Cancer stem cells. *N Engl J Med.* 2006; 355:1253–1261. [PubMed: 16990388]

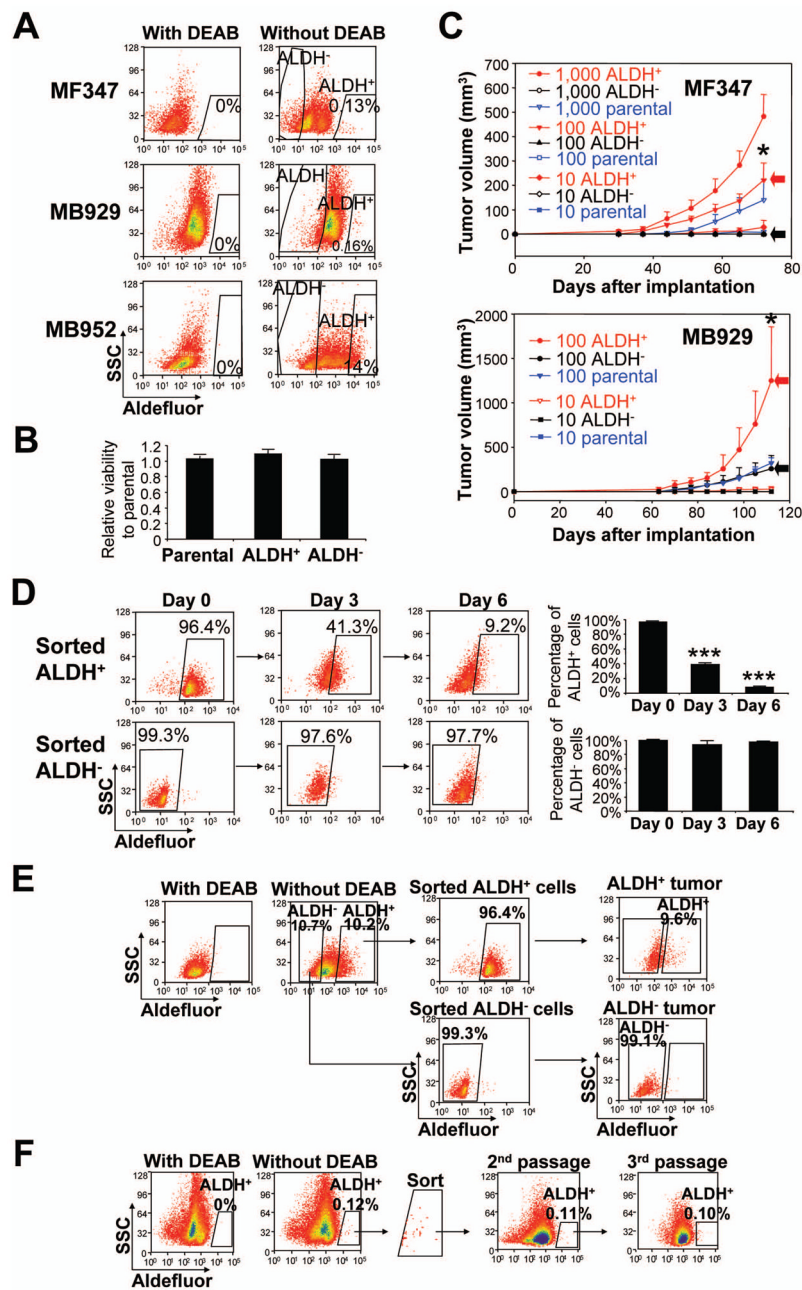


Figure 1.

ALDH⁺ human melanoma cells possess cancer stem cell properties. (A) Representative Aldefluor[®] analysis in primary (MF347) and metastatic (MB929 and MB952) melanomas. Control samples incubated with the inhibitor, DEAB, were used to ensure identification of ALDH⁺ and ALDH⁻ cells. (B) Viability of parental, ALDH⁺ and ALDH⁻ cells *in vitro*. Sorted parental, ALDH⁺ and ALDH⁻ cells from xenografted MB347 tumor were cultured in RPMI-1640 medium with 10% fetal bovine serum, and analyzed by CellTiter 96[®] AQueous One Solution Cell Proliferation Assay 5 days later. (C) Tumorigenesis of xenografted patient tumors (MF347 and MB929) in NOD/SCID mice. Tumor growth curves were plotted for the numbers of engrafted cells (1000, 100, and 10 cells) and for each subpopulation (ALDH⁺, ALDH⁻ and parental). Red and black arrows depict tumor growth from 100

ALDH⁺ cells and 100 ALDH⁻ cells, respectively. Data represent mean \pm SEM (n=4). *, $P < 0.05$ compared with ALDH⁻. **(D)** Differentiation of ALDH⁺ and ALDH⁻ cells *in vitro*. Sorted ALDH⁺ and ALDH⁻ cells from xenografted MB1009 tumor were cultured in RPMI-1640 medium with 10% fetal bovine serum, and analyzed by Aldefluor[®] assay on days 0 (immediately after sorting), 3 and 6. *Left panel*, representative FACS analysis. *Right panel*, percentage of ALDH⁺ (*upper*) and ALDH⁻ (*lower*) cells on days 0, 3 and 6. ***, $P < 0.001$ compared with Day 0. **(E)** Differentiation of ALDH⁺ and ALDH⁻ cells *in vivo*. Sorted ALDH⁺ and ALDH⁻ cells from xenografted MB1009 tumor were implanted into NOD/SCID mice and the developing tumors from ALDH⁺ cells (ALDH⁺ tumor) and those from ALDH⁻ cells (ALDH⁻ tumor) were analyzed by Aldefluor[®] assay. **(F)** Serial transplantation of ALDH⁺ cells from xenografted MF347 tumor. One thousand ALDH⁺ cells were implanted each time in NOD/SCID mice and the developing tumors were analyzed by Aldefluor[®] assay.

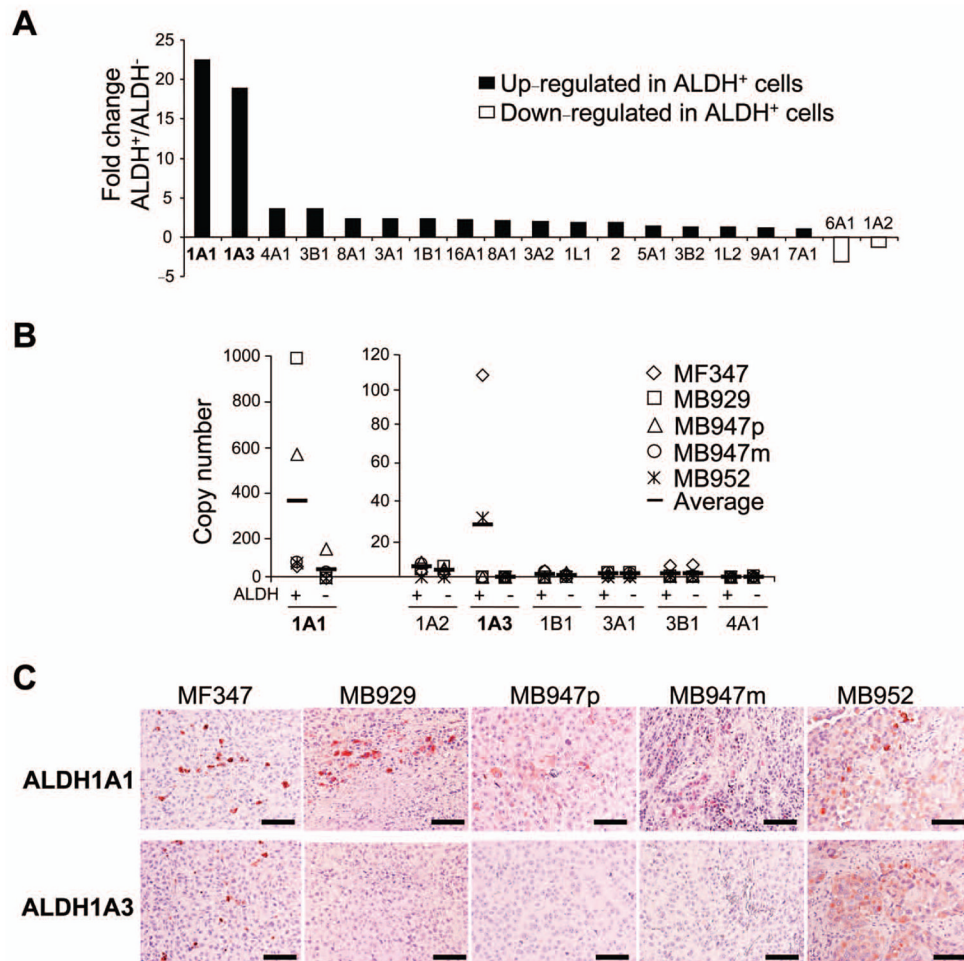


Figure 2. Expression of ALDH isoforms in human melanoma tumors. **(A)** Fold change in 19 ALDH isoforms in ALDH⁺ cells relative to ALDH⁻ cells by microarray analysis. Xenografted patient tumors (MF347, MB929 and MB947m) were analyzed. Isoforms with fold change > 15.0 are emphasized in bold. **(B)** Copy number of representative human ALDH isoforms analyzed by qRT-PCR. mRNAs of ALDH⁺ and ALDH⁻ subpopulations obtained from xenografted patient tumors (MF347, MB929, MB947p, MB947m and MB952) were analyzed. Copy number was counted and determined by standard curve analysis. **(C)** Immunohistochemistry of ALDH1A1 (upper panel) and ALDH1A3 (lower panel) in representative melanoma specimen from patients. Scale bar = 100 μ m.

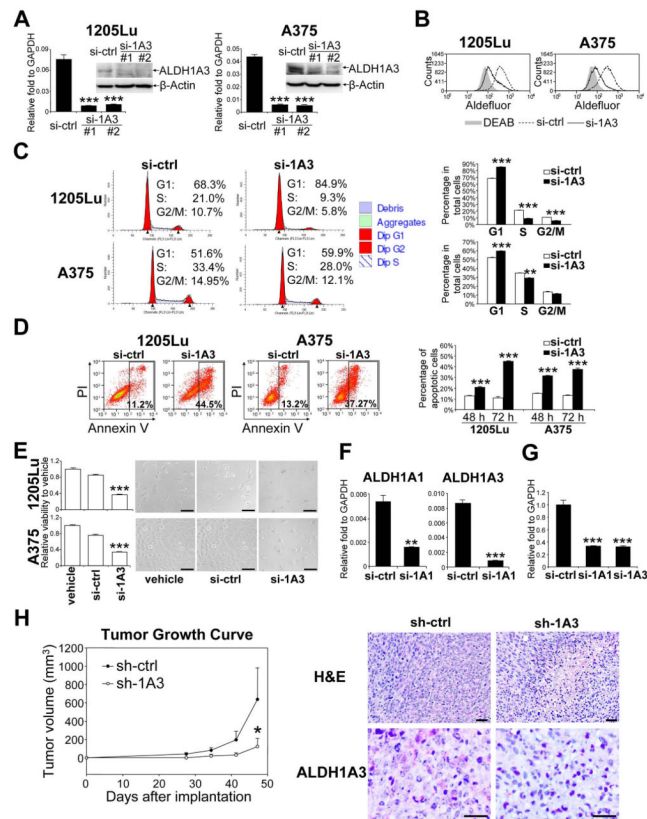


Figure 3.

Biological effect of silencing ALDH1A in ALDH⁺ human melanoma cells. (A) Levels of ALDH1A3 mRNA after siRNA transfection in ALDH⁺ cells from 1205Lu (*left panel*) and A375 (*right panel*) cells. GAPDH and β -actin were used as internal controls for qRT-PCR and Western blot analysis, respectively. Two specific siRNAs (#1 and #2) were used. si-ALDH1A3-#1 (si-1A3-#1) was used for the rest of experiments (Figure 3, B–G). Data represent mean \pm SEM (n=3). ***, $P < 0.001$ compared with control siRNA (si-ctrl). (B) Aldefluor[®] analysis 72 hours after silencing ALDH1A3 in ALDH⁺ 1205Lu and ALDH⁺ A375 melanoma cells. Gray shadow, DEAB control; dashed line, control siRNA (si-ctrl); solid line, ALDH1A3 siRNA (si-1A3). (C) Cell cycle analysis of ALDH⁺ 1205Lu and ALDH⁺ A375 cells at 48 hours after silencing ALDH1A3. *Left panel*, representative histograms. *Right panel*, percentage of cells. G1, Gap1 phase; S, Synthesis phase; G2/M, Gap2 or Mitosis phase. Data represent mean \pm SEM (n=3). **, $P < 0.01$; ***, $P < 0.001$ compared with si-ctrl. (D) Apoptotic cell death of ALDH⁺ 1205Lu and ALDH⁺ A375 cells after ALDH1A3 knockdown. *Left panel*, representative FACS analysis at 72 hours. Annexin V-positive cells were gated as apoptotic. *Right panel*, Annexin V-positive apoptotic cells at 48 and 72 hours. Data represent mean \pm SEM (n=3). ***, $P < 0.001$ compared with control si-ctrl. (E) Cell viability analysis (*left panel*) and bright-field microscopic images (*right panel*) of ALDH⁺ 1205Lu and ALDH⁺ A375 cells 72 hours after ALDH1A3 knockdown. Viability was analyzed by CellTiter-Glo[®] Luminescent Cell Viability Assay. Scale bar = 100 μ m. Data represent mean \pm SEM (n=4). ***, $P < 0.001$ compared with control siRNA (si-ctrl). (F) qRT-PCR analysis of ALDH1A and ALDH1A3 mRNA after transfection of si-ALDH1A1-#1 (si-1A1) and si-ALDH1A3-#1 (si-1A3) in ALDH⁺ xenografted patient tumor cells from MB952 (n=3). Expression levels were normalized to GAPDH. Data represent mean \pm SEM (n=3). **, $P < 0.01$; ***, $P < 0.001$ compared with control siRNA (si-ctrl). (G) Cell viability of ALDH⁺ MB952 cells 72 hours after ALDH1A1 and ALDH1A3

knockdown. Viability was analyzed by CellTiter-Glo[®] Luminescent Cell Viability Assay. Data represent mean \pm SEM (n=4). ***, $P < 0.001$ compared with si-ctrl. **(H)** *Left panel*, tumor growth curves of transfected cells. ALDH⁺ 1205Lu melanoma cells were transfected with GFP-expressing plasmid: sh-control (sh-ctrl) or sh-ALDH1A3 (sh-1A3). GFP-positive cells were sorted and implanted intradermally into NOD/SCID mice. Tumor size was measured weekly. Data represent mean \pm SEM (n=4). *, $P < 0.05$ compared with shRNA control. *Right panels*, representative H&E-stained tumor sections (*right upper panel*) and ALDH1A3-stained tumor sections (*right lower panel*) from ALDH⁺ 1205Lu cells transfected with control shRNA (sh-ctrl) and ALDH⁺ 1205Lu cells transfected with sh-ALDH1A3 (sh-1A3). Scale bar = 100 μ m.

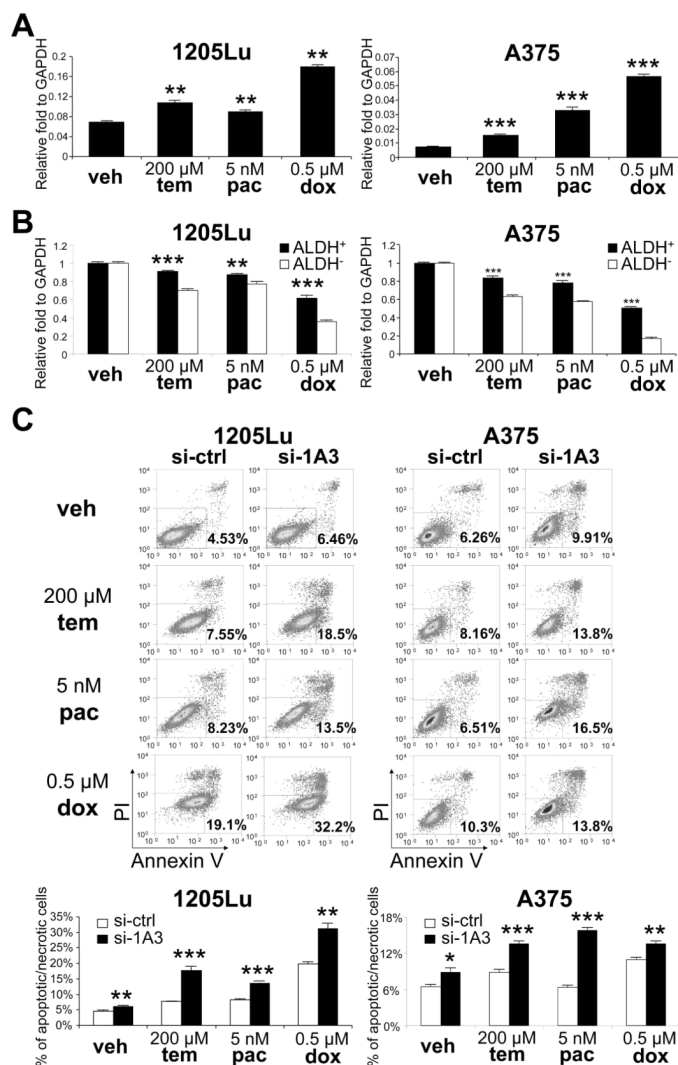


Figure 4. Drug resistance of ALDH⁺ and ALDH⁻ cells. (A) Levels of ALDH1A3 mRNA after treatment of 1205Lu (*left panel*) and A375 (*right panel*) cells with vehicle (veh), temozolomide (tem), paclitaxel (pac) or doxorubicin (dox). Expression levels were normalized to GAPDH. Data represent mean \pm SEM (n=3). **, $P < 0.01$; ***, $P < 0.001$ compared with vehicle treatment. (B) Viability of ALDH⁺ and ALDH⁻ cells from 1205Lu (*left panel*) and A375 (*right panel*) cells after 48 hours of treatment with vehicle (veh), temozolomide (tem), paclitaxel (pac) or doxorubicin (dox). Viability was analyzed by CellTiter-Glo[®] Luminescent Cell Viability Assay. Data represent mean \pm SEM (n=3). **, $P < 0.01$; ***, $P < 0.001$ compared with ALDH⁻ cells. (C) Apoptotic and necrotic cell death of ALDH⁺1205Lu and ALDH⁺A375 cells after transfection of control si-RNA (si-ctrl) or si-ALDH1A3 (si-1A3), treated with vehicle (veh), temozolomide (tem), paclitaxel (pac) or doxorubicin (dox) for 24 hours. *Upper panels*, representative FACS analysis. Annexin V- and/or PI-positive cells were gated as dead cells. *Lower panel*, Annexin V and/or PI-positive cells at 24 hours. Data represent mean \pm SEM (n=3). *, $P < 0.05$; **, $P < 0.01$; ***, $P < 0.001$ compared with vehicle treatment.

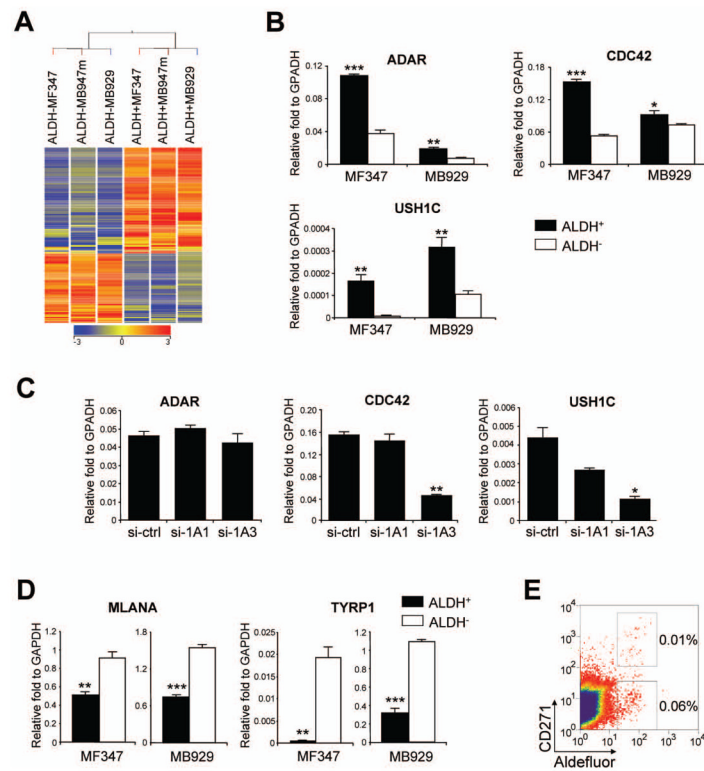


Figure 5. Profiling of ALDH⁺ and ALDH⁻ cells. **(A)** Supervised hierarchical clustering of 147 differentially expressed transcripts between ALDH⁺ and ALDH⁻ cells from xenografted patient melanomas (MF347, MB929 and MB947m). Colored spots indicate upregulated (red) or downregulated (blue) genes from microarray analysis. **(B)** qRT-PCR validation of differentially expressed genes. cDNAs of ALDH⁺ and ALDH⁻ subpopulations were obtained from xenografted patient tumors (MF347 and MB929). Expression levels were normalized to GAPDH. Black and white bars represent expression in ALDH⁺ cells and ALDH⁻ cells, respectively. Data represent mean \pm SEM (n=3). *, $P < 0.05$; **, $P < 0.01$; ***, $P < 0.001$ compared with ALDH⁻ cells. **(C)** qRT-PCR analysis of ADAR, CDC42, and USH1C after siRNA silencing of ALDH1A1 (si-1A1) and ALDH1A3 (si-1A3) in ALDH⁺ xenografted patient melanoma cells from MB952. Expression levels were normalized to GAPDH. Data represent mean \pm SEM (n=3). *, $P < 0.05$; **, $P < 0.01$ compared with transfection of control siRNA (si-ctrl). **(D)** qRT-PCR analysis of melanocyte differentiation antigens, MLANA and TYRP1. cDNAs of ALDH⁺ and ALDH⁻ subpopulations were obtained from xenografted patient tumors (MF347 and MB929). Expression levels were normalized to GAPDH. Data represent mean \pm SEM (n=3). **, $P < 0.01$; ***, $P < 0.001$ compared with ALDH⁻ cells. **(E)** Representative flow cytometric analysis of melanoma tumor (MF348) stained for CD271 and ALDH enzymatic activity.

Table 1

Tumorigenicity and self-renewal of ALDH⁺ cells in NOD/SCID and NSG mice

Melanoma cells	Tumor ID	Tumor development ^a			TIC frequency ⁻¹ (95% CI) ^b	P value ^c
		1,000	100	10		
		(# tumors / # implantation sites)				
ALDH ⁺	MF347	4/4	4/4	1/4		
	MB929	ND	4/4	1/4		<1e ⁻¹² (vs ALDH ⁻)
	MB947p	2/4	3/4	ND		
	MB947m	ND	3/4	1/4		0.0004 (vs Parental)
	MB952	1/1	1/1	ND		
	MB1009	5/5	3/4	ND		
All ALDH ⁺	12/14	18/21	3/12	150 (90–270)		
ALDH ⁻	MF347	0/4	0/4	0/4		
	MB929	ND	2/4	0/4		
	MB947p	2/4	0/4	ND		
	MB947m	ND	0/4	0/4		
	MB952	0/1	0/1	ND		
	MB1009	1/5	0/4	ND		
All ALDH ⁻	3/14	2/21	0/12	2,910 (1,190–7,120)		
Parental	MF347	4/4	1/4	0/4		
	MB929	ND	4/4	0/4		
	MB947p	2/4	0/4	ND		
	MB947m	ND	2/4	0/4		
	MB952	1/1	0/1	ND		
	MB1009	0/1	0/4	ND		
All Parental	7/10	7/21	0/12	520 (280–970)		

B

Cell type	Tumor ID	2 nd passage		3 rd passage	
		Tumor development ^a	TIC frequency ⁻¹ (95% CI) ^b	Tumor development ^a	TIC frequency ⁻¹ (95% CI) ^b
		1,000	100	1,000	100
		(# tumors / # implantation sites)			
	MF347	4/4	4/4	4/4	ND
	MB947p	4/4	ND	4/4	ND
ALDH ⁺ from ALDH ⁺ tumors	MB1009	4/4	ND	4/4	ND
	All ALDH ⁺	12/12	4/4	12/12	<663
			< 155		< 2e ⁻¹⁰⁰ (vs ALDH ⁻)
	MF347				
	MB947p	0/4	ND		
ALDH ⁻ from ALDH ⁻ tumors	MB1009	0/4	ND		
	All ALDH ⁻	0/8	> 2,670		

C

Melanoma cells	Mouse strain	Tumor development ^a		TIC frequency ⁻¹ (95% CI) ^b		P value ^c	
		1,000	10	1,000	10	1,000	10
		(# tumors / # implantation sites)					
	NOD/SCID	MF347	4/4	4/4	1/4	100 (40–220)	1
		MB952	4/4	1/4	0/4		5.65e ⁻⁹
ALDH ⁺	NSG	MF347	ND	4/4	1/4	100 (40–220)	0.016
		MB952	ND	1/4	0/4		
	NOD/SCID	MF347	0/4	0/4	0/4	8,370 (1,180–59,170)	0.136
		MB952	1/4	0/4	0/4		
ALDH ⁻	NSG	MF347	ND	1/4	0/4	830 (120–5,860)	
		MB952	ND	0/4	0/4		

^aTumor initiating capacity of ALDH⁺, ALDH⁻ and parental human melanoma cells in NOD/SCID mice. Tumor growth was monitored for up to 24 weeks after injection of 1000, 100, and 10 cells from xenografted patient tumors (MF347, MB929, MB947p, MB947m, MB947n, MB952 and MB1009).

^bTumor development = (# tumors developed by 24 weeks)/(# sites of initial implantation).

^cThe TIC frequency was calculated by L-Cal Software (with 95% confidence intervals).

- ^cProbability of a difference between groups was determined by chi-square analysis. *P* value represents comparison of TIC frequency in ALDH⁻ or parental cells with that in ALDH⁺ cells. Tumor initiating capacity of ALDH⁺ and ALDH⁻ human melanoma cells serially implanted in NOD/SCID mice. Tumor growth was monitored for up to 24 weeks after injection of 1000 and 100 cells from xenografted patient tumors (MF347, MB947p and MB1009).
- ^aTumor development = (# tumors developed by 24 weeks)/(# sites of initial implantation).
- ^bThe TIC frequency was calculated by L-Calc Software (with 95% confidence intervals).
- ^cProbability of a difference between groups was determined by chi-square analysis. *P* value represents comparison of TIC frequency in ALDH⁻ with that in ALDH⁺ cells. Tumor initiating capacity of ALDH⁺ and ALDH⁻ human melanoma cells in NOD/SCID mice and NSG mice. Tumor growth was monitored for up to 24 weeks after injection of 1000, 100, and 10 cells from xenografted patient tumors (MF347 and MB952).
- ^aTumor development = (# tumors developed by 24 weeks)/(# sites of initial implantation).
- ^bThe TIC frequency was calculated by L-Calc Software (with 95% confidence intervals).
- ^cProbability of a difference between groups was determined by chi-square analysis. *P* value represents comparison of TIC frequency in NOD/SCID mice and NSG mice in the same cells (i.e., ALDH⁺ cells or ALDH⁻ cells).
- ^dProbability of a difference between groups was determined by chi-square analysis. *P* value represents comparison of TIC frequency in ALDH⁻ with that in ALDH⁺ cells in the same mouse strain (i.e., NOD/SCID mice or NSG mice).
- ND: not determined

Table 2

List of 147 genes (fold > 5.0, $p < 0.05$) differentially expressed between ALDH⁺ and ALDH⁻ human melanoma cells in xenografted patient melanomas (MF347, MB929 and MB947m)

Category	Upregulated in ALDH ⁺ cells (99)	Downregulated in ALDH ⁺ cells (48)
Known stem cell genes	<i>ADAR</i> (negative regulation of apoptosis, DNA/RNA binding) <i>ALDH1A3</i> (retinoic acid biosynthetic process) <i>CCNB3</i> (cell cycle, cell division) <i>CDC42</i> ^{***} (regulation of mitosis, maintenance of cell polarity) <i>DACH1</i> (regulation of organogenesis) <i>FGF6</i> (growth factor activity) <i>FOXP1</i> (sequence specific DNA binding, developmental process)	<i>HOXC6</i> (embryonic skeletal system development, anterior/posterior pattern formation) <i>HOXD9</i> (skeletal muscle tissue development, anterior/posterior pattern formation)
Genes potentially associated with stem cell function	<i>ACVR1B</i> [*] (G1/S transition of mitotic cell cycle) <i>BRUNOL4</i> (germ cell development, embryo development) <i>IFNAR2</i> ^a (cell proliferation) <i>KIF11</i> (cell cycle, mitosis) <i>LIF</i> (cell proliferation, growth factor activity) <i>NBR2</i> ^a (cell growth) <i>PRKCZ</i> [*] (anti-apoptosis, cell proliferation) <i>PRKD2</i> (cell survival, cell proliferation) <i>RAD17</i> [*] (DNA repair, DNA replication) <i>RECQL5</i> (DNA repair) <i>REGLA</i> [*] (positive regulation of cell proliferation) <i>RELI</i> ^{***} (DNA repair, anti-apoptosis) <i>USH1C</i> (G2/M transition of mitotic cell cycle)	<i>ACHE</i> ^{****} (apoptosis) <i>BCL2L12</i> (apoptosis) <i>CCDC64</i> ^a (nervous system development) <i>CNTFR</i> [*] (promote neuron cell differentiation) <i>HMX2</i> ^a (neuron differentiation, nervous system development) <i>MGLL</i> (promote tumor growth) <i>SOHLH2</i> (cell differentiation) <i>STAB1</i> (negative regulation of angiogenesis)
Transporter	<i>ABCG1</i> ^a , <i>GABRB2</i> , <i>GGA1</i> ^{**} , <i>NPTX1</i> ^a , <i>SLC35F1</i> , <i>TRPC3</i> ^a	<i>CPNE6</i> [*] , <i>SLC2A11</i> [*]
Protein binding	<i>ANKMY1</i> , <i>ANKS6</i> , <i>ARPM2</i> , <i>BTBD3</i> , <i>CHRFAM7A</i> , <i>CLDN4</i> , <i>DPP3</i> [*] , <i>EPB41</i> [*] , <i>FAM128B</i> ^{***} , <i>GFAP</i> [*] , <i>HYAL2</i> , <i>MICALL2</i> , <i>NLRP9</i> , <i>PLIN</i> , <i>PPP2R1B</i> , <i>SPSB4</i> [*] , <i>TBCEL</i> , <i>TMEM118</i> , <i>TMEM63B</i> ^a	<i>KRT18</i> [*] , <i>LRRRC48</i> ^{**} , <i>NCF1B</i> ^a , <i>TBCE</i> ^a
Regulation of transcription	<i>MED8</i> , <i>PIAS2</i> [*] , <i>TAOK2</i> ^a , <i>ZNF155</i> , <i>ZNF454</i> , <i>ZNF75A</i> [*]	<i>CDYL</i> [*] , <i>FOXF2</i> , <i>ONECUT1</i> , <i>SETD7</i> ^{**} , <i>USP21</i> , <i>ZNF175</i> ^a
Signal transduction	<i>GNAT1</i> , <i>GPR37L1</i> ^{***} , <i>BDKRB2</i> , <i>DZIP1L</i> , <i>EDEM3</i> , <i>IL18R1</i> , <i>IL28RA</i> ^{***} , <i>PLCB1</i> , <i>PLEKHG5</i> , <i>RAB15</i> [*] , <i>RCAN1</i> ^a , <i>ROPN1B</i> , <i>TAGAP</i> [*]	<i>GNB5</i> [*] , <i>HIF3A</i> ^{**} , <i>ITPKA</i> ^{**} , <i>OR10H5</i> , <i>OR14I1</i> , <i>OR1S1</i> , <i>PRKACB</i> , <i>TLR3</i> , <i>TLR8</i>
Metabolic process	<i>AMT</i> [*] , <i>ANXA8</i> ^a , <i>APOL1</i> [*] , <i>ASRGL1</i> , <i>BDH1</i> ^a , <i>MMP1</i> , <i>MTUS1</i> , <i>PIGH</i> [*] , <i>PPP1R3C</i> [*] , <i>PTGS2</i> [*] , <i>RNASE1</i> [*] , <i>THRSP</i> [*] , <i>UNQ9391</i>	<i>FJ32569</i> , <i>SPINK9</i> , <i>TLL3</i> [*]
Cell adhesion	<i>CNTN4</i> , <i>FERMT3</i> ^{**} , <i>FEZ1</i> , <i>ITGA3</i> ^a	<i>PCDH11X</i> [*] , <i>SCARF1</i> [*]
Other functions	<i>DUSP27</i> , <i>FAM13C1</i> , <i>GAGES5</i> [*] , <i>GM127</i> ^a , <i>LCAP</i> , <i>MAGEF1</i> , <i>MAPK8IP3</i> , <i>MS4A13</i> , <i>PGBD2</i> , <i>PTRH1</i> , <i>PRICKLE2</i> , <i>RNF128</i> , <i>PTRH1</i> , <i>SAMD10</i> ^a , <i>TOP3A</i> , <i>TMEM174</i> [*] , <i>UBTD2</i> ^{***} , <i>UBXD5</i> [*]	<i>ARVP6125</i> , <i>CMYA3</i> , <i>DONSON</i> [*] , <i>EP400NL</i> , <i>GLUL</i> ^{**} , <i>KIAA0284</i> ^a , <i>MGC42367</i> ^a , <i>PFN4</i> , <i>PGM5P2</i> ^a , <i>PRY2</i> , <i>SCYL3</i> , <i>SSR2</i> ^a

Genes with predicted RARE element between upstream (-10 kb) to downstream (+1 kb) of TSS were emphasized with underline.

*, **, *** or **** represent 1, 2, 3 or 4 RARE elements, respectively.

^aRARE element was not analyzed, since the location from -10 kb to 1 kb of TSS for the gene can not determined by PromoSer.